International Journal of Biophysics 2018, 8(1): 9-15
DOI: 10.5923/j.biophysics.20180801.02

Synthesis, X-Ray Structure and Molecular Docking Analysis of Two Novel 1,2,4,5-Tetrasubstituted Imidazole Derivatives

Ratika Sharma[1], A. Jayashree[2], B. Narayana[2], B. K. Sarojini[3], C. Ravikumar[4], S. Murugavel[5], Sumati Anthal[1], Rajni Kant[1,*]

[1]X-ray Crystallography Laboratory, Department of Physics, University of Jammu, Jammu Tawi, India
[2]Department of Studies in Chemistry, Mangalore University, Mangalagangotri, India
[3]Department of Studies in Chemistry-Industrial Chemistry Section, Mangalore University, Mangalagangotri, India
[4]Thanthai Periyar EVR Government Polytechnic College, Vellore, Tamilnadu, India
[5]Department of Physics, Thanthai Periyar Government Institute of Technology, Vellore, Tamilnadu, India

Abstract Imidazole derivatives **I** [1-(3,5-Difluoro-4-methylphenyl)-2-(4-fluorophenyl)-4,5-diphenyl-1*H*-imidazole and **II** 2-(4-fluorophenyl)-4,5-diphenyl-1-(4-trifluoro)-phenyl-1H-imidazole] have been synthesized by using multicomponent reaction(MCR). The compounds (**I** & **II**) are crystallized in the monoclinic space group *I2/a* and in triclinic space group *P-1* with unit cell parameters a = 22.1693(7), b= 8.1636(6), c=25.7250(19) Å, β = 112.526(9)° and a = 9.2427(6), b = 13.4381(9), c =19.7520(4) Å, α= 90.464(5)°, β = 99.530(5)°, γ=106.210(6)° respectively. The complexes have been characterized by single crystal X-ray crystallographic analysis which revealed the asymmetric unit of the compound **II** contains two crystallographically independent molecules with almost similar geometries. The crystal structures were solved by Direct Methods and refined by Full Matrix least squares procedure. The C-H …F [inter-molecular and intra-molecular] interactions plays an important role in stabilizing the crystal packing. Molecular docking studies were used to identify the inhibitory activity against fungal protein cyctochrome P450 14 α demethylase enzyme.

Keywords Imidazole, Crystal structure, Direct method, Intermolecular and intramolecular interactions, X-ray analysis, Molecular docking

1. Introduction

Synthesis of multisubstituted imidazoles through multi-component reactions has got much attraction since they are an important class of pharmaceutical compounds and attractive targets in medicinal chemistry. They exhibit a wide spectrum of biological activities such as anti-inflammatory [1], antibacterial [2], antitumor, anti-diabetic [3]. The incorporation of the imidazole nucleus is an important synthetic strategy in drug discovery and finds tremendous applications in the treatment of several diseases [4]. It has been reported that these derivatives show various pharmacological activities such as analgesic [5], anti-depressants [6], antiviral [7], anticancer [8], anti-leishmanial [9] etc. In view of the numerous biological, pharmacological and material properties associated with 1,2,4,5-tetra substituted imidazoles, we report the synthesis and crystal structure of two novel 1,2,4,5-tetrasubstituted imidazole derivatives along with their docking studies.

Infections caused by fungus are one of the major health problem faced by human beings presently. The occurrence of primary and adaptable nature of fungal infections persists to increase precipitously because of the increased number of immune compromised patients who are affected with tuberculosis, AIDS, cancer and organ transplantation [10-12]. Universal antifungal agents can be normally grouped based on their action mechanism in pathogenic fungi, primarily in cell membrane, cell wall and intracellular action [13]. Hence, constant search for antifungal agents on new targets or new mechanism of action is essential.

Drug discovery programs are oriented to the search for lead structures. Virtual screening and molecular docking constitute great alternatives to find hit compounds. Azoles are the chief choice of drugs for the treatment of fungal infection high therapeutic index [14]. These facts directed us to quest for novel azoles lead compounds with more structural specificity for inhibit fungal enzymes. In this paper,

* Corresponding author:
rkant.ju@gmail.com (Rajni Kant)
Published online at http://journal.sapub.org/biophysics

molecular docking studies were carried out against the fungal protein cytochrome P450 sterol 14DM CYP-51 of C. albicans (PDB Id: 1E9X) [15] with the synthesized imidazole derivatives. The binding energy and interactions were found using AutoDock Vina [16]. The docking results were compared with the standard drug, clotrimazole, an antifungal medication which is sold in the brand name canesten to treat a wide variety of fungal infections like vaginal yeast infections, diaper rash, oral thrush, etc.

2. Experimental

2.1. Synthesis and Mechanism

A mixture of benzil (1 mmol), substituted amine (1 mmol), aryl aldehyde (1 mmol), ammonium acetate (1 mmol) and ZnO nanoparticles (0.1 mmol) in glacial acetic acid was heated at 60°C under stirring for around 2 hrs. The progress of the reaction was monitored by TLC. After completion of the reaction, the mixture was cooled to room temperature. The reaction mixture was then poured into cold water. The solid separated was filtered by suction to afford crude product. The pure tetra-substituted imidazoles were obtained by further recrystallization from ethanol/water. Crystal of the purified products was generated in acetone/water. The complete reaction scheme is presented in Figure 1.

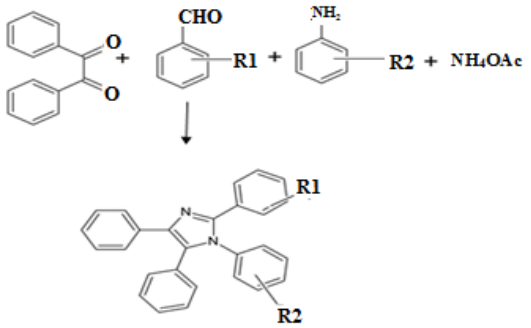

Figure 1. Reaction scheme

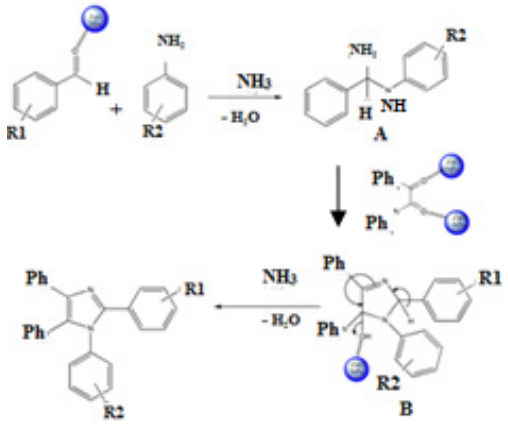

Figure 2. A plausible mechanism for the formation of tetrasubstituted imidazoles

A plausible mechanism for the synthesis of the tetrasubstituted imidazole involves the formation of intermediate [A] by the reaction of an aldehyde, substituted aniline and ammonium acetate in the presence of ZnO nanoparticles as catalyst [Figure 2]. Intermediate [A] condenses with benzil to form intermediate [B], which in turn liberates a water molecule to form tetrasubstituted imidazole. ZnO nano particle is a highly efficient catalyst which can form complex with benzaldehyde and benzil. This probably facilitates the formation of intermediate [A] and [B]. Higher catalytic activity of ZnO nanoparticles may be attributed to the surface area which is available for greater adsorption of reactants on its surface.

2.2. X-ray Data Collection and Structure Refinement

X-ray intensity data of both the compounds **I** and **II** (size; 0.30 X 0.20 X 0.10 mm) having well-defined crystal morphology were collected at 293(2) *K* on *X'calibur* CCD area-detector X-ray Diffractometer [17] equipped with Mo*Kα* radiation (λ=0.71073 Å). The cell dimensions were determined by the least-squares fit of angular settings of 1810(**I**), and 3330(**II**) reflections in the θ range 3.7 to 26.7°(**I**) and 4.1 to 26.0°(**II**), respectively. $I > 2\sigma(I)$ criterion were employed to the unique data sets. Data were corrected for Lorentz and Polarization factors. The structures were solved by direct methods using SHELXS97 [18]. All non-hydrogen atoms of the molecules of both the structures were located from the best E-map and Full-matrix least-squares refinement was carried out using SHELXL97 [18]. The hydrogen atoms were geometrically fixed and allowed to ride on the corresponding non-H atoms. Atomic scattering factors were taken from International Tables for X-ray Crystallography (1992, Vol. C, Tables 4.2.6.8 and 6.1.1.4). **CCDC 1484506** and **1479887** contains the supplementary crystallographic data for **I** and **II** respectively. The crystallographic data are summarized in Table 1.

Table 1. Crystal Data and Other Experimental Details of Com pound **I** and **II**

Compound	**I**	**II**
Empirical formula	$C_{28}H_{19}F_3N_2$	$C_{28}H_{18}F_4N_2$
Formula weight	440.45	458.44
Radiation, Wavelength	Mo *K*α, 0.71073 Å	Mo *K*α, 0.71073 Å
Unit cell volume	4298.4(6) Å^3	2319.2(3) Å^3
No. of molecules per unit cell, Z	8	4
F(000)	824	944
θ range for entire data collection	3.50< θ < 25.00°	3.50< θ < 25.00°
Reflections collected / unique	3774 /2203	15723/8118
Reflectionsobserved I > 2σ(I))	1810	3245
Final R-factor	0.0789	0.0774
wR(F2)	0.2731	0.2000
Rint	0.0345	0.0457
Rsigma	0.0645	0.1074
Goodness-of-fit	1.058	0.954

Some selected bond lengths and angles which play an important role in collating the structural properties of these structures with some analogous ones are presented in Table 2 and Table 3. An ORTEP [19] view of the molecules with atomic labeling is shown in Figure 3 and Figure 4. The geometrical calculations were performed by using the PLATON [20] and PARST [21] software.

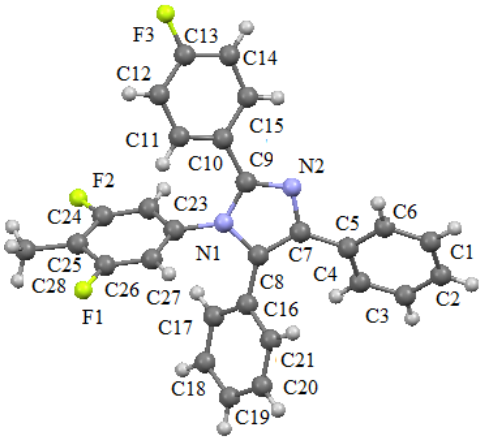

Figure 3. ORTEP view of the compound **I** with displacement ellipsoids at the 40% probability level. H atoms shown as small spheres

Table 2. Selected Bonds Lengths (Å) and Angles (°) for Compound (**I**)

Bond Lengths (Å)		Bond Angles (°)	
N1-C8	1.397(5)	C9-N1-C8	107.0(3)
N1-C9	1.372(5)	C9-N2-C7	127.3(3)
N2-C7	1.371(5)	F1-C13-C12	118.7(4)
N2-C9	1.318(5)	F1-C13-C14	118.3(3)
F2-C26	1.256(2)	F2-C26-C27	114.1(5)
F3-C26	1.267(2)	F3-C24-C26	109.7(1)

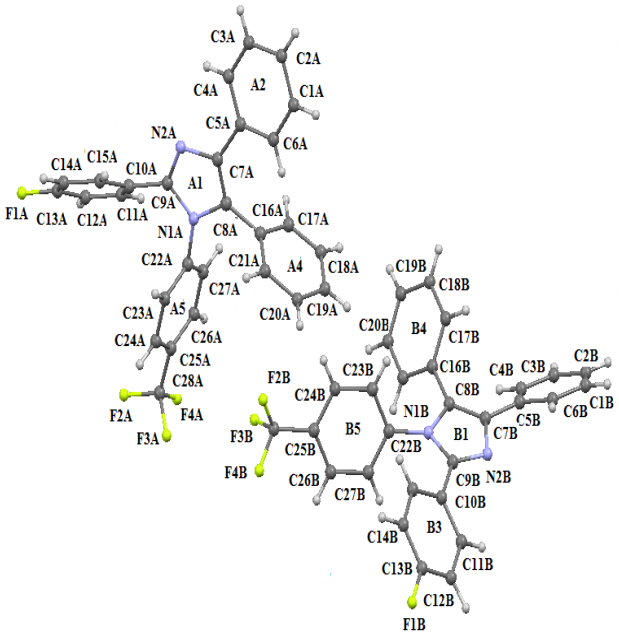

Figure 4. ORTEP view of compound **II** with displacement ellipsoids at the 40% probability level. H atoms shown as small spheres of arbitary radii

Table 3. Selected Bonds Lengths (Å) and Angles (°) for Compound (**II**)

Molecule A

Bond Lengths (Å)		Bond Angles (Å)	
N1A-C8A	1.397(5)	C7A-N2A-C9A	107.0(3)
N1A-C9A	1.372(5)	C7A-C8A-C16A	105.9 (3)
N2A-C7A	1.371(5)	C8A-N1A-C22A	126.9 (3)
N2A-C9A	1.318(5)	N2A-C7A-C5A	119.4 (4)
F2A-C28A	1.256(2)	C9A-N2A-C7A	105.9 (3)
F3A-C28A	1.267(2)	C8A-N1A-C9A	107.3 (3)

Molecule B

Bond Lengths (Å)		Bond Angles (Å)	
N1B-C8B	1.388(5)	C7B-N2B-C9B	107.0(3)
N1B-C9B	1.378(5)	C7B-C8B-C16B	106.4 (3)
N2B-C7B	1.395(5)	C8B-N1B-C22B	127.3 (3)
N2B-C9B	1.324(5)	N2B-C7B-C5B	119.4 (4)
F2B-C28B	1.342(2)	C9B-N2B-C7B	106.4 (3)
F3B-C28B	1.318(2)	C8B-N1B-C9B	107.0 (4)

2.3. Molecular Docking Studies

Molecular docking provides useful facts about drug receptor interactions and is frequently used to compute the binding orientation of small molecule drug candidates to their protein targets in order to calculate the affinity and activity of the small molecule. In our study, molecular docking is carried out using AutoDock Vina to find out the binding energy and interactions of synthesized imidazole derivatives with the protein, cytochrome P450 sterol 14DM CYP-51 of C. albicans (PDB Id: 1E9X) downloaded from Protein Data Bank (http://www.rcsb.org). The removing of hydrogen atoms and crystallized ligand structures of the protein along with addition of polar hydrogens were carried out using AutoDock Tools and the same were saved as PDBQT file. Ligand was also taken and saved in PDBQT file using ADT. The binding centre values based on active site present in protein with grid center coordinates (X= -17.143, Y= -6.199, Z= 64.493) and grid box size (x = 20, y = 20, z = 20). The docking results were viewed with Discovery Studio, 2015 [22].

3. Results and Discussion

3.1. 1-(3,5-Difluoro-4-Methylphenyl)-2-(4-Fluorophenyl)-4,5-Diphenyl-1H-Imidazole(I)

The X-ray analyses reveal that both the molecules belong to the same series of compounds with different substitutions at the two phenyl rings. In compound **I** all bond lengths and angles are normal [23] and comparable with those reported for related compounds [24, 25]. All the rings in the molecule are planar. The three phenyl rings bonded to the imidazole at the position C7, C9, C8 and N1 are inclined to the imidazole ring at the dihedral angle 48.48(1), 24.10(2), 27.26(3) and 70.95(3)° respectively. The architecture of the crystal structure is determined mainly by one intermolecular

[C-H…F] and one intramolecular [C-H…F] hydrogen bonds. C28 acts as the hydrogen bond donar in both inter and intra hydrogen bonds. C28-H28C…F1 interactions results in the formation of chains along the *b*-axis [Figure 5]. These chains of molecules are packed together to form two-dimensional network running along *ac- plane* [Figure 6].

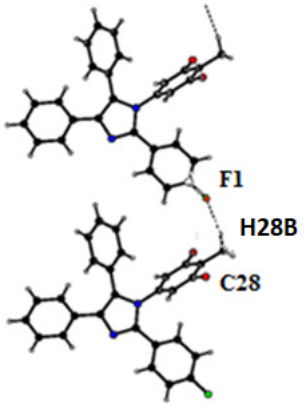

Figure 5. Part of the crystal structure, showing the formation of chains. The dashed lines show intermolecular C-H…F hydrogen bond

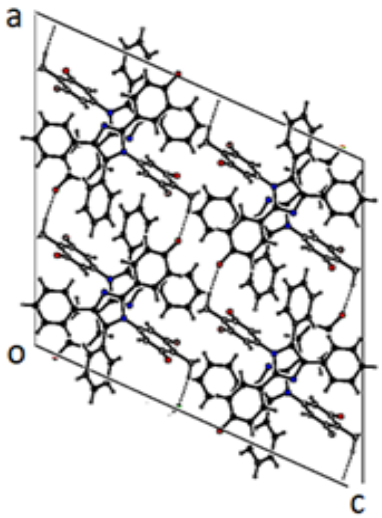

Figure 6. The packing arrangement of compound **I** viewed in the *ac*-plane

3.2. 2-(4-Fluorophenyl)-4,5-Diphenyl-1-(4-Trifluoro)-Phenyl-1H-Imidazole(II)

The asymmetric unit of the compound **II** comprises of two crystallographically independent molecules, (A and B) with almost similar geometries. All the bond lengths and bond angles are normal [23-25] and in close agreement with each other except to those involving triflurometlhyl group (F2/ F3/ F4/ C28) which shows significant variations in the two symmetry-independent molecules *viz* F1A-C28A= 1.263(8) Å; F1B-C28B= 1.342(5) Å, F3A-C28A= 1.211(8) Å; F3B-C28B= 1.318(5) Å & F4A-C28A=1.211(8); F4B-C28B=1.316(5) Å. The imidazole ring exhibits normal geometry [23] and is planar in both the asymmetric-independent molecules with maximum deviation for the atom C8A [0.0068 (5) Å] in molecule A and C7B [0.0032 (4) Å] in molecule B. The fluorine atom F1 has been found to lie in the plane of the atoms C10-C15 in both the molecules. The planarity of the fluorine atom has also been indicated by the value torsion angle F1A-C13A-C14A-C15A=179.7(2)° and F1B-C13B-C14B-C15B=179.2(2)°. The triflurometlhyl ring is also coplanar with the plane of the ring defined by the atom C25 to C24. The architecture of the hydrogen bonding is determined mainly by two C-H…F and one C-H…N intra-molecular hydrogen bonds [Table 4]. The packing view of the molecules in compound **II** in the *bc-plane* is presented in the Figure 7.

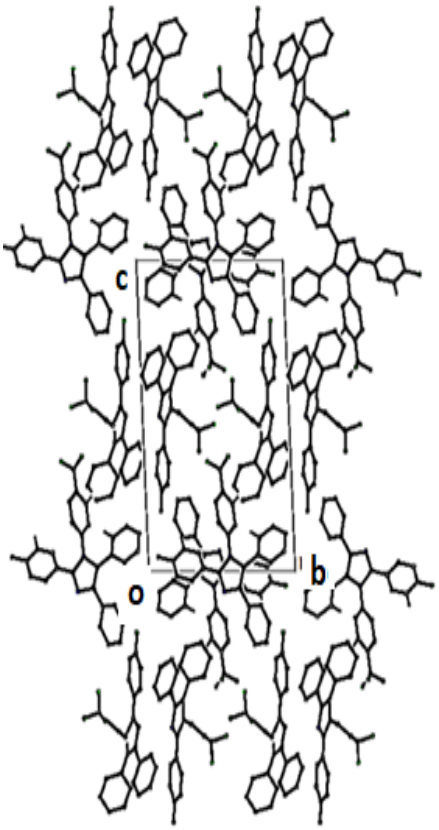

Figure 7. Packing view of compound **II**

Table 4. Geometry of Intra and Inter-Molecular Interactions for Compound I and Compound II

Compound I

D–H…A	D–H(Å)	H…A(Å)	D…A(Å)	D–H…A(°)
C28-H28…F3	0.96	2.33	2.718(9)	103
C28-H28C…F1^{i}	0.96	2.19	3.126(7)	166

Symmetry Code: i) x+1/2, -y+1, +Z

Compound II

D–H…A	D–H(Å)	H…A(Å)	D…A(Å)	D–H…A(°)
C14A-H14A…F1B	0.93	2.52	3.26(6)	138
C21B-H21B…N2B	0.93	2.49	2.82(6)	102
C24B-H24B…F3B	0.93	2.43	2.74(6)	100

3.3. Molecular Docking Analysis (I & II)

Literature survey reveals that azole derivatives are good antifungal agents and they show good antifungal activity against cytochrome P450 sterol 14DM CPY51 of C. albicans, which is the best target to analyze the antifungal activity of the synthesized imidazole derivatives. The imidazole derivatives compounds (**I**) and (**II**) were docked with 14 α demethylase enzyme and was compared with the standard drug clotrimazole. Figure 8 shows the ligand-protein binding interactions of compound (**I**), compound (**II**) and Clotrimazole to 1E9X binding site. Table 5 shows the docked interactions and binding energy scores of compound (**I**), compound (**II**) and clotrimazole with the binding site of the target protein 14α-demethylase. The docking studies of synthesized compounds with 1E9X protein showed that the docking energy of -10.9 kcal/mol for compound(**I**)-1E9X complex and -11.3 kcal/mol for Compound (**II**)-1E9X complex, which are higher than that of standard drug clotrimazole-1E9X complex (-9.0 kcal/mol). The compound (**I**)-1E9X complex is stabilized by two hydrogen bonds, one halogen bond and one hydrophobic interaction. The residues LYS97 and HIS101 interact with the atoms F2 and F3 of the ligand, respectively, through hydrogen bond interactions. Also, a peculiar halogen bond is observed between the fluorine atom F1 and the residue ALA73. Further, a hydrophobic π-π interaction is observed between imidazole ring of the ligand and a six-membered ring of the residue TYR76.

The compound (**II**)-1E9X complex is stabilized by two hydrogen bonds, one halogen bond and one electrostatic interaction. The residues LYS97 and ALA73 interact with the atoms F3 and F2 of the ligand, respectively, through hydrogen bond interactions. Also, a halogen bond is observed between the fluorine atom F2 and the residue GLN72. Further, an intermolecular cation-π interaction is observed between HZ3 atom of the residue LYS97 and trifluoro ring of the ligand. The Clotrimazole-1E9X complex is stabilized by one hydrogen bond with residue GLN72 and one hydrophobic sigma-π interaction with residue ALA256.

As we know that, the occurrence of more number of interactions in the docking complexes will enhance the binding affinity and bioactivity of the compounds. As evident from Table 5, our synthesized compounds, show more interactions with the target protein 1E9X and also possess high docking energy score than the standard drug. Hence, the compounds **I** and **II** may be treated as vital inhibitors of 14α demethylase enzyme and as a drug for fungal diseases.

Table 5. Docking Energy and Interaction of Compound I and II, Clotrimzole with Target Protein 1E9X

Target protein	Inhibitor	Docking Energy (kcal/mol)	Interactions	Distance (Å)	Bonding	Bonding Type
(PDB ID: 1E9X)	Compound (I)	-10.9	(LYS97) Z-HZ1…F2	3.598	Hydrogen	H-bond
			(HIS101) ND1-HD1…F3	4.028	Hydrogen	H-bond
			(ALA73) O…F1	3.448	Halogen	Halogen-bond
			(TYR76) π…π (imidazolering)	4.267	Hydrophobic	π -π bond
	Compound (II)	-11.3	(LYS97) NZ-HZ2…F3	3.915	Hydrogen	H-bond
			(ALA73) N-H…F2	3.848	Hydrogen	H-bond
			(GLN72) OE1…F2	3.579	Halogen	Halogen -bond
			(LYS97) NZ-HZ3…π (trifluoro ring)	4.066	Hydrogen Electrostatic	Cation-π bond
	Clotrimazole	-9.0	(GLN72) NE2-HE21…N2	3.721	Hydrogen	H-bond
			(ALA256) CB-HB3…π (C9...C14ring)	2.766	Hydrophobic	σ-π bond

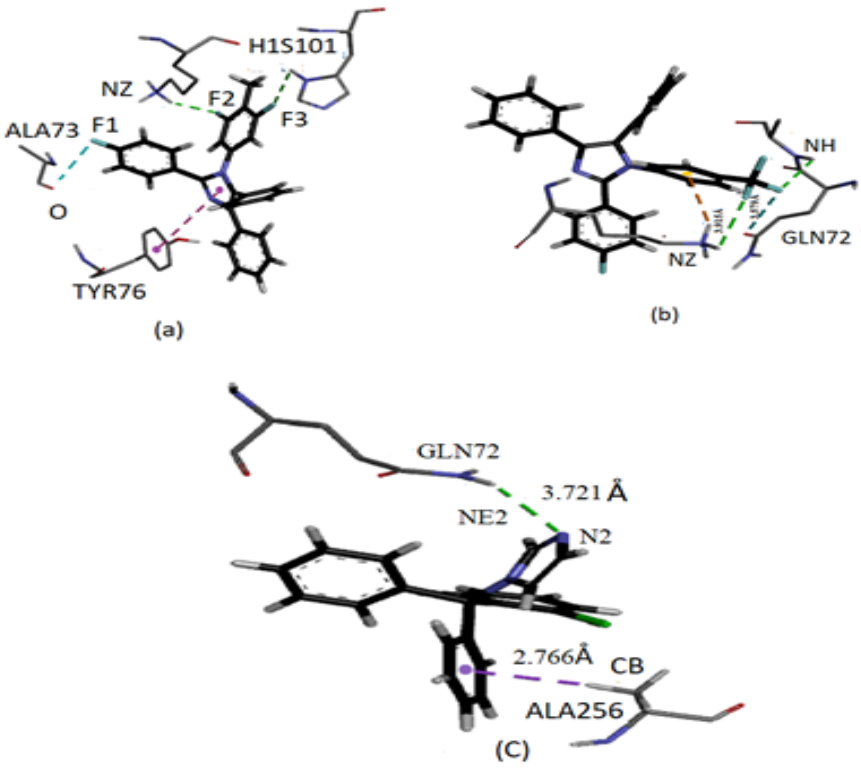

Figure 8. Ligand-protein binding interactions of compounds (I), (II) and standard drug lotrimazole to 1E9

4. Conclusions

Imidazole derivatives have occupied a unique place in the field of medicinal chemistry and is inclusion forms an important synthetic strategy in drug discovery. They are currently the most widely used insecticides in the world and are widely used for pest control in agriculture. Because of the wide application of these compound three biologically active Tetra-substituted imidazole derivatives (**I&II**) were synthesized by the multi-component reaction which provide us most powerful platform to access diversity as well as complexity in a limited number of reaction steps. The molecular structures have been determined by using X-ray diffractometer. The result of the single-crystal X-ray structure analysis establishes the structural aspects of these compounds. None of the structure exhibits any significant intermolecular interaction. In compound **I** the molecular packing is stabilized by inter molecular hydrogen bond. The packing of the other compound has been established by the presence of intra-molecular hydrogen bonds and *van der waals* forces.

ACKNOWLEDGEMENTS

One of the authors (Rajni Kant) acknowledges the Indian Council of Medical Research (Research Project No: BIC/12(14)/2012) and the Department of Science and Technology (Research Project No EMR/2014/000467) for the financial support.

REFERENCES

[1] Misono, M., 2001, Unique acid catalysis of heteropoly compounds (heteropolyoxometalates) in the solid state, M. Chem. Commun., 13, 1141-1152.

[2] Antolini M., Bozzoli, A., Ghiron, C., Kennedy, G., Rossi T., and Ursini, A., 1999, Analogues of 4,5-bis(3,5-dichlorophenyl)-2-trifluoromethyl-1H-imidazole as potential antibacterial agents, Bioorg. Med. Chem. Lett., 9, 1023-1028.

[3] Nanterment, P. G., Barrow, J. C., Lindsley, S. R., Young, M., Mao, S., Carroll, S., Bailey, C., Bosserman, M., Colussi, D., McMasters, D. R., Vacca, J. P., and Selnick, H. G., 2004, Imidazole acetic acid TAFI a inhibitors: SAR studies centered around the basic P(1)(') group, Bioorg. Med. Chem. Lett., 14, 2141-2145.

[4] Shalini, K., Sharma, P. K., and Nitin, K., 2010, Imidazole and its biological activities: A review, Der Chemica Sinica, 1, 36-47.

[5] Puratchikodya, A., and Doble, M., 2007, Antinociceptive and antiinflammatory activities and QSAR studies on 2-substituted-4,5-diphenyl-1H-imidazoles, Bioorg. Med. Chem. Lett., 15, 1083-1090.

[6] Hadizadeh, F., Hosseinzadeh, H., Sadat Motamed-Shariaty, V., Seifi M., and Kazemi, S., 2008, Synthesis and antidepressant activity of N-substituted imidazole-5-carboxamides in forced swimming test model, Iran J Pharm Res., 7, 29-33.

[7] Sharma, D., Narasimhan, B., Kumar, P., Judge, V., Narang, R., De Clercq E., and Balzarini, J., 2009, Synthesis, antimicrobial and antiviral evaluation of substituted imidazole derivatives, Eur. J. Med. Chem., 44, 2347-2353.

[8] Refaat, H. M., 2010, Synthesis and anticancer activity of some novel 2-substituted benzimidazole derivatives. Eur. J. Med. Chem., 45, 2949-2956.

[9] Bhandari, K., Srinivas, N., Marrapu, V. K., Verma, A., Srivastava, S., and Gupta, S., 2010, Synthesis of substituted aryloxy alkyl and aryloxy aryl alkyl imidazoles as antileishmanial agents, Bioorg. Med. Chem. Lett., 20, 291-293.

[10] Andriole, A.T., 2000, Current and future antifungal therapy: new targets for antifungal therapy, Int. J. Antimicrob. Agents, 16, 317-321.

[11] Dismukes, W. E., 2000, Introduction to Antifungal Drugs, Clin. Infect. Dis., 30, 653-657.

[12] Rostom, S. A., Ashour, H. M., El Razik, H. A., El Fattah Ael, F., and El-Din., N. N., 2009, Azole antimicrobial pharmacophore-based tetrazoles: synthesis and biological evaluation as potential antimicrobial and anticonvulsant agents, Bioorg. Med. Chem., 17, 2410-2422.

[13] Lewis, R. E., 2011, Current concepts in antifungal pharmacology, Mayo Clinic Proceedings, 86, 805.

[14] Mansfield, B. E., Oltean, H.N., Oliver, B.G., Hoot, S. J., and Leyde, S. E., 2010, Azole drugs are imported by facilitated diffusion in Candida albicans and other pathogenic fungi, PLoS Pathog 6, e1001126.

[15] Podust, L. M., Poulos, T. L., and Waterman, M. R., 2001, Crystal Structure of Cytochrome P450 14Alpha -Sterol Demethylase (Cyp51) from Mycobacterium Tuberculosis in Complex with Azole Inhibitors, Proc. Natl. Acad. Sci. USA, 98, 3068-3073.

[16] Trott, O., and Olson, A. J., 2010, Auto Dock Vina: improving the speed and accuracy of docking with a new scoring function, efficient optimization, and multithreading, J Comput Chem., 31, 455-461.

[17] Oxford Diffraction, 2010, CrysAlis PRO, Oxford Diffraction, Yarnton, UK.

[18] Sheldrick, G. M., 2008, A short history of SHELX, Acta Cryst., A64, 112-122.

[19] Farrugia, L. J., 1999, WinGX suite for small-molecule single-crystal crystallography.

[20] Spek, A. L., 2009, Structure validation in chemical crystallography, Acta Cryst., D65, 148-155.

[21] Nardelli, M., 1995, PARST95- an update to PARST: a system of Fortran routines for calculating molecular structure parameters from the result of crystal structure analysis, J. Appl. Cryst., 28, 659.

[22] Discovery Studio 2015, Dassault Systems BIOVIA, Discovery Studio Modelling Environment, Release 4.5, San Diego: Dassault Systems.

[23] Allen, F., Kennard, O., D.G. Watson, D. G., L. Brammer, L., and Orpen, A. G., 1987, Tables of bond lengths determined by X-ray and neutron diffraction. Part1. Bond lengths in Organic compounds, Taylor, R., J. Chem. Soc., Perkin Trans-II, S1-S19.

[24] Gayathri, P., Thiruvalluvar, A., Srinivasan, N., Jayabharathib J., Butcher, R. J. 2010, 2-(4-Fluorophenyl)-1,4,5-triphenyl-1Himidazole, Acta Cryst., E66, o2519.

[25] Viveka, S., M. Prabhuswamy, M., Dinesha, N. K. Lokanath, N. K., and Nagaraja., G. K., 2014, Synthesis Characterization and Crystal Structure of 2-(3,4,5-trimethoxyphenyl)-1-(4-fluorophenyl)-4,5-diphenyl-1*H*-imidazole, Mol. Cryst. Liq. Cryst., 593, 261-270.